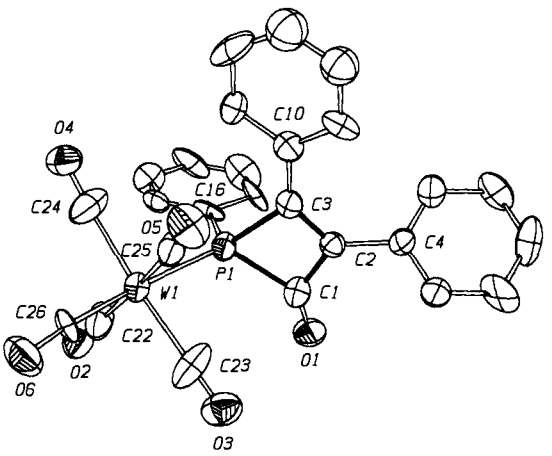

Figure 1. Structure of one molecule of complex **2a**. Thermal ellipsoids are scaled to enclose 50% of the electron density; hydrogen atoms are omitted. Principal bond distances (Å, means between the two units): W-P1, 2.470 (3); P1-C1, 1.93 (1); P1-C3, 1.83 (1); P1-C16, 1.85 (1); C1-O1, 1.16 (1); C1-C2, 1.48 (1); C2-C3, 1.36 (1); C2-C4, 1.52 (1); C3-C10, 1.46 (1); Cphe-Cphe, 1.371 (4); W-C, 2.02-2.06 (1); C-O, 1.134 (6). Selected bond angles (deg, means between the two units): W1-P1-C1, 121.8 (3); W1-P1-C3, 120.5 (3); W1-P1-C16, 121.2 (4); C1-P1-C3, 71.9 (5); P1-C1-C2, 88.8 (7); P1-C3-C2, 97.0 (7); C1-C2-C3, 102.2 (9); Cphe-Cphe-Cphe, 119.9 (2).

phosphorus analogues of unsaturated β-lactams. Thus we have also studied the decomplexation of complex **2a**. We have followed the same general scheme as for the synthesis of 1,2,3-triphenylphosphirene from its P-W(CO)$_5$ complex.[4] In a first step, the P-W bond of **2a** is weakened through oxidation of tungsten by 1 mol of pyridinium tribromide, then the phosphorus ligand is displaced from the brominated complex by 2 mol of 2,2′-bipyridyl. P-Oxidation takes place spontaneously.

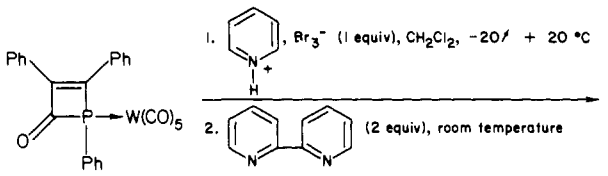

2a

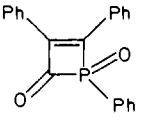

3

The 2,2′-bipyridyl complexes which are present in the crude reaction mixture together with **3** are precipitated by adding ether to the medium. After filtration and evaporation, **3** is recrystallized in a mixture of dichloromethane and hexane.[12] Finally, since the 1,2-dihydrophosphete ring was never structurally characterized before, we decided to perform the X-ray crystal structure analysis of **2a**, which gave the following crystal data: $C_{26}H_{15}O_6PW$, M_w 638.23; triclinic; a = 9.954 (3) Å, b = 24.817 (6) Å, c = 9.824 (3) Å, α = 99.00 (2)°, β = 90.37 (2)°, γ = 97.94 (2)°, U = 2373 Å^3, d_{obsd} = 1.77 ± 0.03 g cm^{-3}, Z = 4, d_{calcd} = 1.786 g cm^{-3}, space group $P\bar{1}$ (No. 2). Mo Kα (0.710 73 Å) radiation was used for cell dimension determination and intensity measurement at -100 °C (cold nitrogen flow); μ = 50.762 cm^{-1}, F_0 = 1232.

Diffraction data were collected in the $\theta/2\theta$ flying step-scan mode with a Philips PW 1100/16 automatic diffractometer at -100 °C, graphite monochromated Mo Kα radiation, and a crystal of dimensions 0.018 × 0.016 × 0.024 cm. Absorption corrections were applied by the numerical integration method (transmission factor 0.89 → 1.10). The structure was solved by the heavy atom method with the Enraf-Nonius SDP/V+1 package on a PDP 11/60 computer. Full-matrix refinement using 4537 reflections having $I > 3\sigma(I)$ converged to conventional agreement factors R_1 and R_2 of 0.047 and 0.079 with anisotropic temperature factors for all non-hydrogen atoms. Hydrogen atoms were introduced by their computed coordinates but not refined.

The asymmetric unit contains two independent W(CO)$_5$(P-C$_3$O(C$_6$H$_5$)$_3$) moieties which are not significantly different from each other. The structure (Figure 1 shows one moiety) consists of discrete molecules with no nonusual intramolecular bonds. Selected geometrical averages between the two molecules are given in the caption of Figure 1.

The insertion of CO in the P-C-C triangle leads to an opening of the intracyclic C-P-C angle from 42.8 (2)° to 71.9 (5)°. The P-C intracyclic bonds are significantly different, the longest being on the carbonyl side, whereas the shortest has a normal value for a P-C single bond. The C=C intracyclic double bond remains well localized between C2 and C3 (molecule 1).

Supplementary Material Available: Listings of atomic positional and thermal parameters and of observed and calculated structure factors (×10) (25 pages). Ordering information is given on any current masthead page.

(12) **3**: yellow solid, mp 130 °C; ^{31}P NMR (CH_2Cl_2) δ +63; ^{13}C NMR (CD_2Cl_2) δ 141.36 (d, ^1J(C-P) = 44.5 Hz, PC(Ph)), 160.46 (d, ^1J(C-P) = 84.3 Hz, PCPh), 180.35 (d, ^2J(C-P) = 70.5 Hz, COCPh), 202.13 (d, ^1J(C-P) = 65.7 Hz, PCO); IR (KBr) ν(P-CO) 1722 cm^{-1}, ν(P=O) 1217 cm^{-1}; mass spectrum (CI, CH_4, ^{184}W), m/e 331 (M + 1, 100%).

(13) Marinetti, A.; Mathey, F.; Fischer, J.; Mitschler, A. *J. Chem. Soc., Chem. Commun.* **1982**, 667.

Long-Distance Electron Transfer in Pentaammineruthenium (Histidine-48)-Myoglobin. Reorganizational Energetics of a High-Spin Heme

Robert J. Crutchley, Walther R. Ellis, Jr., and Harry B. Gray*

Contribution No. 7174, Arthur Amos Noyes Laboratory California Institute of Technology Pasadena, California 91125

Received April 15, 1985

Both the kinetics and thermodynamics of long-distance electron transfer[1,2] have been successfully determined in two ruthenium-modified metalloproteins, a$_5$Ru(His-33)-cytochrome *c* (a = NH$_3$)[1a,b] and a$_5$Ru(His-83)-azurin.[1c,d] In both proteins the electron-acceptor site is buried in the protein interior, and it is inferred from the weak temperature dependence of the electron-transfer rate constant that the reorganizational enthalpy of the low-spin ferriheme[3] or blue copper is very small. An obvious test of the postulated origin of the weak (or lack of) temperature dependence is to examine a system with an acceptor where the inner-sphere reorganizational energy is relatively large, namely, a ruthenium-modified protein containing a high-spin ferriheme. We report here our results on one such semisynthetic system, a$_5$Ru(His-48)-myoglobin (Figure 1).[4,5]

(1) (a) Nocera, D. G.; Winkler, J. R.; Yocom, K. M.; Bordignon, E.; Gray, H. B. *J. Am. Chem. Soc.* **1984**, *106*, 5145-5150. (b) Isied, S. S.; Kuehn, C.; Worosila, G. *J. Am. Chem. Soc.* **1984**, *106*, 1722-1726. (c) Margalit, R.; Kostić, N. M.; Che, C.-M.; Blair, D. F.; Chiang, H.-J.; Pecht, I.; Shelton, J. B.; Shelton, J. R.; Schroeder, W. A.; Gray, H. B. *Proc. Natl. Acad. Sci. U.S.A.* **1984**, *84*, 6554-6558. (d) Kostić, N. M.; Margalit, R.; Che, C.-M.; Gray, H. B. *J. Am. Chem. Soc.* **1983**, *105*, 7765-7767.

(2) Other recent work on long-distance electron transfer in metalloproteins: (a) Ho, P. S.; Sutoris, C.; Liang, N.; Margoliash, E.; Hoffman, B. M. *J. Am. Chem. Soc.* **1985**, *107*, 1070-1071. (b) McLendon, G. L.; Winkler, J. R.; Nocera, D. G.; Mauk, M. R.; Mauk, A. G.; Gray, H. B. *J. Am. Chem. Soc.* **1984**, *106*, 5012-5013. (d) Peterson-Kennedy, S. E.; McGourty, J. L.; Hoffman, B. M. *J. Am. Chem. Soc.* **1984**, *106*, 5010-5012.

(3) Analysis of the oxidized and reduced cytochrome *c* X-ray structures suggests a low theoretical value as well (Churg, A. K.; Weiss, R. M.; Warshel, A.; Takano, T. *J. Phys. Chem.* **1983**, *87*, 1683-1694).

0002-7863/85/1507-5002$01.50/0

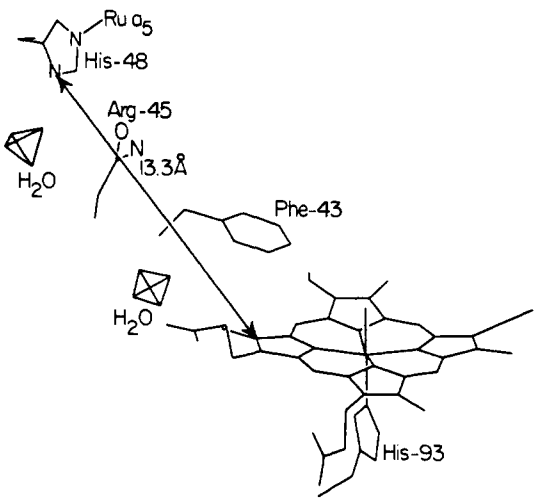

Figure 1. View of selected parts of the molecular skeleton of sperm whale myoglobin with a_5Ru^{3+} bonded to the imidazole of His-48. The closest distance between the a_5Ru^{3+}(His-48) group and the heme is 13.3 Å.

Table I. Thermodynamic Parameters[7,8] for the Reduction of a_5Ru^{3+} and the Heme Site in Native and Modified Mb[a]

thermodynamic parameter	native Mb $Fe^{3+/2+}$	modified Mb $Fe^{3+/2+}$	modified Mb $a_5Ru^{3+/2+}$
$E°$, mV vs. NHE (25 °C)	58.8 ± 2	65.4 ± 2	85.8 ± 2
$\Delta G°$, kcal mol^{-1} (25 °C)	−1.26 ± 0.05	−1.51 ± 0.05	−1.98 ± 0.05
$\Delta S°$, e.u.	−39.1 ± 1.2	−37.6 ± 1.2	4.2 ± 1.2
$\Delta H°$, kcal mol^{-1} (25 °C)	−13.0 ± 0.4	−12.7 ± 0.4	−0.7 ± 0.4

[a] pH 7.0, I = 0.1 M phosphate buffer.

Spectroscopic measurements (UV–visible, CD, EPR, and proton NMR[6]) indicate that the heme site is virtually unperturbed by the a_5Ru^{3+} label. This conclusion is supported by electrochemical results (Table I). The entropy and enthalpy changes associated with reduction of the ferriheme and ruthenium(3+) sites in the myoglobin derivative were determined by using variable-temperature spectroelectrochemistry and differential-pulse polarography, respectively. As the reduction potentials (at 25 °C) for the ruthenium and heme iron sites in the modified protein differ by only 20 mV, the observed rate constant (eq 1) for intramolecular electron transfer between these sites is expected to follow

$$a_5Ru^{3+}(His\text{-}48)Mb(Fe^{3+}) \xrightarrow[e^-]{fast} a_5Ru^{2+}(His\text{-}48)Mb(Fe^{3+}) \underset{k_{-1}}{\overset{k_1}{\rightleftharpoons}} a_5Ru^{3+}(His\text{-}48)Mb(Fe^{2+}) \quad (1)$$

reversible, first-order behavior (i.e., $k_{obsd} = k_1 + k_{-1}$).

Production of a_5Ru^{2+}(His-48)Mb(Fe^{3+}) was achieved by flash photolysis[9] of a solution of the fully oxidized protein derivative and $Ru(bpy)_3^{2+}$ (bpy = 2,2′-bipyridine). EDTA was present in solution to scavenge $Ru(bpy)_3^{3+}$ produced by oxidative quenching.[10] The observed electron-transfer rate closely follows first-order behavior and is independent of protein concentration (5–50-μM range). The sequence of electron-transfer steps is summarized in eq 1. At 25 °C, the forward rate (k_1) is 0.019 ± 0.002 s^{-1} while the reverse rate (k_{-1}) is 0.041 ± 0.003 s^{-1}. The temperature dependences (5–45 °C range) of the forward and reverse rate constants yield $\Delta H_1^{\ddagger}$ and $\Delta H_{-1}^{\ddagger}$ values of 7.4 ± 0.5 and 19.5 ± 0.5 kcal mol^{-1}, respectively (Figure 2).

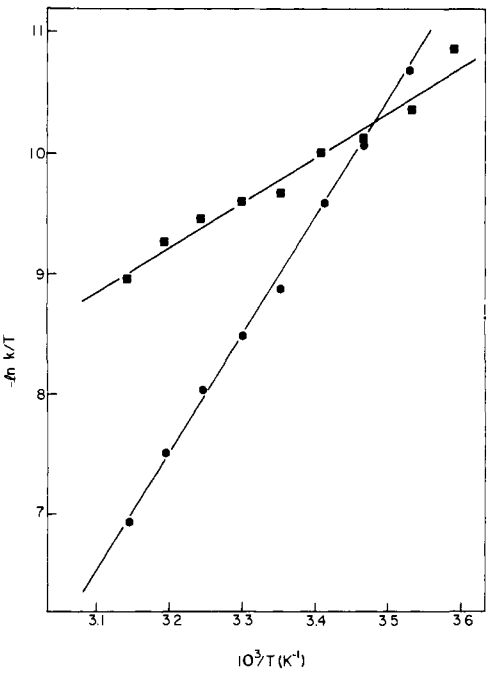

Figure 2. Eyring plots of k_1 (■) and k_{-1} (●). The lines are least-squares fits to the data (pH 7.0, I = 0.1 M).

An additional experiment supports our interpretation of the kinetic behavior of this system. When the flash photolysis solution is saturated with carbon monoxide, a large increase in absorbance at the monitoring wavelength (568 nm)[11] is observed. CO binds to the ferrous heme generated in step k_1 and prevents back electron transfer to produce the ferric heme. The equilibrium step in eq 1 is thus transformed into a dead-end reaction yielding a_5Ru^{3+}(His-48)Mb(Fe^{2+}–CO).

Our work establishes directly that high-spin hemes are much less efficient in long-distance electron transfer than low-spin analogues. After Marcus and Sutin,[12] we estimate the enthalpic reorganizational barrier for the heme in myoglobin to be 20 kcal mol^{-1} (in contrast to the low (7–8 kcal mol^{-1}) reorganizational enthalpy obtained for the low-spin heme in cytochrome c[1a]). X-ray crystallographic studies[13] indicate that reduction of metmyoglobin to deoxymyoglobin results in dissociation of the axial water molecule from the iron atom. This change in ligation most likely accounts for the much larger reorganizational barrier, because

(4) Sigma Type II sperm whale myoglobin (Mb) was reacted with a 15-fold excess of $[Ru(NH_3)_5OH_2](PF_6)_2$ at room temperature (pH 7.0). The reaction was terminated after 30 min by passage of the solution through a Sephadex G-25 gel column. The surface of Mb contains four His residues (12, 48, 81, and 116) that react with a_5Ru^{2+}. After oxidation of the mixture of modified protein, preparative isoelectric focusing (LKB Multiphor, ampholines, and ultrodex) and cation-exchange chromatography (Whatman CM-52 resin) yield all four expected singly modified proteins as well as multiply modified derivatives.

(5) Isolation and characterization of the (His-48)-containing tryptic peptide of a_5Ru^{3+}(His-48)Mb have confirmed the a_5Ru^{3+} attachment site (Shelton, J. B.; Shelton, J. R.; Schroeder, W. A., unpublished results).

(6) Toi, H.; LaMar, G. N.; Margalit, R.; Che, C.-M.; Gray, H. B. *J. Am. Chem. Soc.* **1984**, *106*, 6213–6217.

(7) $Ru^{3+/2+}$ potentials were obtained using nonisothermal differential pulse polarography in the presence of 4,4′-bipyridine. Mb($Fe^{3+/2+}$) potentials were obtained using nonisothermal thin-layer spectroelectrochemistry with $[(NH_3)_6Ru]Cl_3$ present as a redox mediator. Temperature range: 5–45 °C. The electrochemical equipment and procedures are described in ref 1a.

(8) $\Delta S° = (dE°/dT)_p - 15.6$ eu. $\Delta S°$ is the entropy for the complete cell reaction adjusted to the NHE scale (i.e., $S°_{H^+}$ is assigned a value of zero).

(9) The flash photolysis apparatus has been described previously (Milder, S. J.; Goldbeck, R. A.; Kliger, D. S.; Gray, H. B. *J. Am. Chem. Soc.* **1980**, *102*, 6762–6764).

(10) The $Ru(bpy)_3^{2+}$/EDTA photoreducing system is discussed in ref 1a. Control experiments involving native Mb show that the partial reduction of the ferric heme by EDTA-derived radicals is very rapid and does not interfere with the collection of intramolecular electron-transfer rate data.

(11) The monitoring wavelength, 568 nm, is an isosbestic point of Mb and MbCO absorption spectra.

(12) See: Marcus, R. A.; Sutin, N. *Inorg. Chem.* **1975**, *14*, 213–216. Since the reactants are fixed spatially, $\Delta H^{\ddagger} = \Delta H^{*}$. We use eq 9 and assume α = 0. ΔH^{*}_{Ru} is approximated at 6.9 kcal mol^{-1}, the value for the $[(NH_3)_5Rupy]^{3+/2+}$ self-exchange.

(13) Takano, T. *J. Mol. Biol.* **1977**, *110*, 537–568; 569–584.

the axial ligands (His and Met) in cytochrome c[14] are retained upon reduction of the iron center.

Acknowledgment. We thank Steve Mayo for Figure 1. R.J.C. acknowledges a postdoctoral fellowship from the Natural Sciences and Engineering Research Council of Canada. This research was supported by National Science Foundation Grant CHE82-18502.

(14) Takano, T.; Dickerson, R. E. *J. Mol. Biol.* **1981**, *153*, 79-94; 95-115.

Protonation of Molybdenum(II) and Tungsten(II) Bis(alkyne) Complexes: Formation of η^4-C_4R_4H Ligands

J. R. Morrow, T. L. Tonker, and J. L. Templeton*

W. R. Kenan, Jr., Laboratory
Department of Chemistry, University of North Carolina
Chapel Hill, North Carolina 27514

Received February 22, 1985

Protonation of a metal-bound alkyne carbon in $M(R^1C_2R^2)_2(S_2CNR_2)_2$ complexes[1] (M = Mo or W, R^1 = R^2 = Ph, R = Et; M = Mo, R^1 = Ph, R^2 = H, R = Me) with HBF_4 induces an oxidative coupling of the C_2 moieties to form an η^4-C_4R_4H ligand. Stoichiometric addition of HBF_4 to $M(PhC_2Ph)_2(S_2CNEt_2)_2$ (M = Mo, W) in CH_2Cl_2 followed by precipitation and trituration with Et_2O yields $[M(\eta^4\text{-}C_4Ph_4H)(S_2CNEt_2)_2][BF_4]$.[2] The carbene carbon (C_1) resonates at low field (W, 270.0 ppm, $^1J_{WC}$ = 84 Hz; Mo, 279.8 ppm) while the protonated carbon (C_4) is found at much higher field in the ^{13}C NMR spectrum (W, 76.9 ppm, $^1J_{CH}$ = 154 Hz; Mo, 83.5 ppm, $^1J_{CH}$ = 157 Hz). The two intervening carbons of the MC_4 ring are also bound to the metal and exhibit shifts between 114 and 122 ppm for both metals. Both ^1H and ^{13}C NMR indicate that $Mo(PhC_2H)_2(S_2CNMe_2)_2$ adds acid at a terminal acetylenic carbon and undergoes head-to-tail coupling to yield $[Mo(\eta^4\text{-}C(Ph)C(H)C(Ph)CH_2)(S_2CNMe_2)_2]^+$, with a phenyl substituent on the carbene carbon, as the only isolated isomer.[3]

Reaction of $[W(\eta^4\text{-}C_4Ph_4H)(S_2CNEt_2)_2][BF_4]$ with aqueous NEt_3 in CH_2Cl_2 results in substitution of one dithiocarbamate by an oxide ligand to form a neutral $W(O)(\eta^4\text{-}C_4Ph_4H)(S_2CNEt_2)$ complex (see Scheme I). Purification of the crude product by chromatography on Florisil separated two isomers: **a**, eluted with CH_2Cl_2, dark orange, unique ^1H at 4.05; **b**, eluted with Et_2O/CH_2Cl_2 (1/100), dark gold, unique ^1H at 5.77 ppm. Both isomers exhibit NMR spectra characteristic of the η^4-C_4Ph_4H ligand and an intense W=O infrared absorption.[4] The chemical shift difference of 1.7 ppm for the unique proton of the C_4Ph_4H ligand in the two isomers is comparable to differences seen for syn and anti positions of π-allyl or π-butadiene ligands.[5] The anti position of the terminal proton in isomer **a** (vide infra) was anticipated from the higher ^1H chemical shift relative to the analogous proton in isomer **b**, and we tentatively assign a syn proton location to the C_4Ph_4H ligand in **b**. Isomer **a** can be cleanly converted to **b** by heating in wet acetonitrile for several hours at 54 °C.

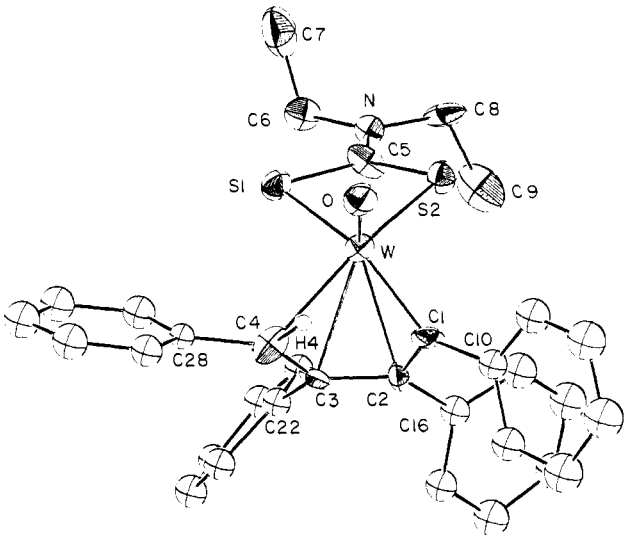

Figure 1. ORTEP diagram showing the atomic labeling scheme for $W(O)(\eta^4\text{-}C_4Ph_4H)(S_2CNEt_2)$. The position of H4 is a calculated one, and it is drawn in only to assist in visualizing the C_4Ph_4H ligand. The thermal ellipsoids are drawn at the 40% probability level.

Scheme I

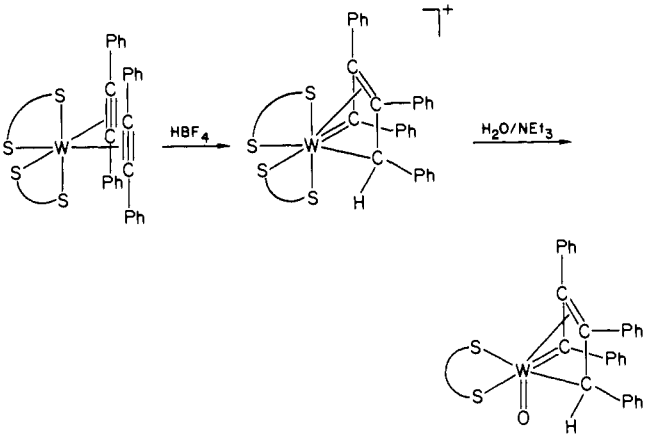

(1) Molybdenum reagents were synthesized by literature methods.[1a,b] The tungsten bisalkyne reagent was synthesized by reflux of $W(CO)(PhC_2Ph)(S_2CNEt_2)_2$[1c,d] with excess diphenylacetylene in methanol for 8 h followed by alumina chromatography with toluene as eluant and recrystallization from a methylene chloride/hexanes solvent mixture. (a) Herrick, R. S.; Templeton, J. L. *Organometallics* **1982**, *1*, 842. (b) McDonald, J. W.; Newton, W. E.; Creedy, C. T. C.; Corbin, J. L. *J. Organomet. Chem.* **1975**, *92*, C25. (c) Ricard, L. Weiss, R.; Newton, W. E.; Chen. G. J.-J.; McDonald, J. W.; *J. Am. Chem. Soc.* **1978**, *100*, 1318. (d) We used an alternate synthetic route: Morrow, J. R.; Tonker, T. L.; Templeton, J. L. *Organometallics* **1985**, *4*, 745.

(2) $[W(\eta^4\text{-}C_4Ph_4H)(S_2CNEt_2)_2][BF_4]$: ^1H NMR ($CDCl_3$) δ 7.62-6.52 (m, 20, C_6H_5), 4.27-3.73 (m, 8, CH_2), 4.14 (s, 1, CHPh), 1.55 (m, 6, CH_3), 1.38, 1.24 (t, 6, CH_3); ^{13}C NMR ($CDCl_3$) δ 270.0 (s, $^1J_{W\text{-}C}$ = 84 Hz, =CPh), 200.4, 199.4 (s, S_2CNEt_2), 136.5-125.8 (C_6H_5), 121.1, 114.4 (s, =CPhCPhCPhCHPh), 76.9 (d, $^1J_{CH}$ = 154 Hz, CHPh), 48.0, 47.0 (t, $^1J_{CH}$ = 140 Hz, CH_2), 12.5, 12.8, 13.4 (q, $^1J_{CH}$ = 129 Hz, CH_3); IR (CH_2Cl_2) ν_{CN} 1530 cm^{-1}; $[Mo(\eta^4\text{-}C_4Ph_4H)(S_2CNEt_2)_2][BF_4]$: ^1H NMR (CD_2Cl_2) δ 7.73-6.53 (m, 20, C_6H_5), 4.71 (s, 1, CHPh), 4.21-3.36 (m, 8, CH_2), 1.47 (t, 6, CH_3), 1.35-1.12 (m, 6, CH_3); ^{13}C NMR ($CDCl_3$) δ 279.8 (s, =CPh), 199.7, 197.6 (s, S_2CNEt_2), 135.9-127.6 (C_6H_5), 122.1, 113.7 (s, =CPhCPhCPhCHPh), 83.5 (d, $^1J_{CH}$ = 157 Hz, CHPh), 47.4, 46.7 (t, $^1J_{CH}$ = 140 Hz, CH_2), 13.5, 12.7 (q, $^1J_{CH}$ = 130 Hz, CH_3); IR (CH_2Cl_2) ν_{CN} 1524 cm^{-1}.

(3) $[Mo(\eta^4\text{-}C(Ph)C(H)C(Ph)CH_2)(S_2CNEt_2)_2][BF_4]$: ^1H NMR ($CDCl_3$) δ 7.61-7.20 (m, 10, C_6H_5), 7.4 (approximate chemical shift estimated from homonuclear decoupling experiments, =CPhCHCPhCH$_2$), 4.58, 3.25 (dd, 2, ^2J = 4, ^4J = 1 Hz, =CPhCHCPHCH$_2$), 3.74 (s, 6, CH_3), 3.33, 2.94 (s, 6, CH_3); ^{13}C NMR ($CDCl_3$) δ 272.2 (s, =CPh), 202.9, 200.9 (s, S_2CNEt_2), 136.3-126.0 (C_6H_5), 94.4 (d, $^1J_{CH}$ = 173 Hz, =CPhCHCPhCH$_2$), 62.0 (t, $^1J_{CH}$ = 156 Hz, CH_2), 45.2-39.2 (q, overlapping, CH_3); IR (CH_2Cl_2) ν_{CN} 1550 cm^{-1}. Anal. Calcd for $MoS_4N_2C_2H_{25}BF_4$: Mo, 15.27; N, 4.46; C, 42.04; H, 4.02. Found: Mo 15.51; N, 4.99; C, 41.02; H, 4.36.

(4) $W(O)(C_4Ph_4H)(S_2CNEt_2)$ (**a** isomer): ^1H NMR ($CDCl_3$) δ 7.42-6.58 (m, 20, C_6H_5), 4.05 (s, 1, $^2J_{WH}$ = 21 Hz, CHPh), 3.94-3.52 (m, 4, CH_2), 1.38, 1.25 (t, 6, CH_3); ^{13}C NMR ($CDCl_3$) δ 266.5 (s, =CPh), 204.5 (S_2CNEt_2), 144.2-123.2 (C_6H_5 and one =CPhCPhCPhCHPh), 119.1 (s, one of =CPhCPhCPhCHPh), 68.0 (d, $^1J_{CH}$ = 136, $^1J_{WC}$ = 53 Hz, CHPh), 46.1, 45.3 (t, $^1J_{CH}$ = 135 Hz, CH_2), 12.7, 12.5 (q, $^1J_{CH}$ = 127 Hz, CH_3); IR (KBr) ν_{CN} 1510, ν_{WO} 957 cm^{-1}; $W(O)(C_4Ph_4H)(S_2CNEt_2)$ (**b** isomer): ^1H NMR ($CDCl_3$) δ 7.45-6.70 (m, 20, C_6H_5), 5.77 (s, 1, $^1J_{WH}$ = 9 Hz, CHPh), 3.89-3.32 (m, 4, CH_2), 1.33, 1.15 (t, 6, CH_3); ^{13}C NMR ($CDCl_3$) δ 271.8 (s, =CPh), 207.1 (s, S_2CNEt_2), 145.4-123.5 (C_6H_5 and =CPhCPhCPhCHPh), 76.8 (d, $^1J_{CH}$ = 144 Hz, CHPh), 45.8, 45.4 (t, $^1J_{CH}$ = 135 Hz, CH_2), 12.5, 12.2 (q, $^1J_{CH}$ = 128 Hz, CH_3); IR (KBr) ν_{CN} 1525, ν_{WO} 955 cm^{-1}.

(5) (a) Green, M. L. H.; Nagy, P. L. I. *Adv. Organomet. Chem.* **1964**, *2*, 325. (b) Pettit, R.; Emerson, G. F. *Adv. Organomet. Chem.* **1964**, *1*, 1. (c) Collman, J. P.; Hegedus, L. S. "Principles and Applications of Organotransition Metal Chemistry"; Oxford University Press: Mill Valley, CA, 1980.

0002-7863/85/1507-5004$01.50/0